JOURNAL OF SPACECRAFT AND ROCKETS
Vol. 45, No. 4, July–August 2008

Explosive-Hazard Analysis for Reusable Launch Vehicles in On-Pad Environments

Christopher J. Freitas* and Sidney Chocron†
Southwest Research Institute, San Antonio, Texas 78238-5166

DOI: 10.2514/1.33392

A computational modeling approach or method was developed for simulating 1) the release of the fuel and oxidizer from a launch vehicle, 2) the subsequent mixing of the fuel and oxidizer in the local on-pad environment of the launch vehicle, 3) the explosive potential or yield for the mixture plume, and 4) the detonation of the plume and the resulting collateral damage. The method uses a set of computer codes: specifically, a computational fluid dynamics code to predict vapor plume formation, a chemical-thermodynamic equilibrium code to predict vapor plume yield potential, and a hydrocode to predict explosion intensity and collateral damage. This method was successfully applied to the simulation of candidate reusable launch vehicles to assess crew-escape performance.

Nomenclature

S = fragment size, m or in.
K_c = material fracture toughness, MPa · $m^{0.5}$ or ksi · $in.^{0.5}$
ρ = material density, kg/m^3 or $lbm/in.^3$
c = material speed of sound, m/s or in./s
$\dot{\varepsilon}$ = strain rate, s^{-1}

I. Introduction

THE catastrophic failure of a reusable launch vehicle (RLV) during launch poses a significant engineering problem for the design of crew-escape systems. The explosive-hazard potential of the RLV changes during the various phases of the launch due to engine operational states and local environmental conditions. The explosive-hazard potential in the on-pad environment is characterized by the potential release and formation of a gas-phase mixture in an oxidizer-rich environment, whereas the hazard during the ascent phase is dominated by the boundary layer and wake flow formed around the vehicle and the interaction of a released fuel plume with the exhaust jets. To more effectively address crew escape in these potentially explosive environments, a computational analysis effort was undertaken. This study was part of the TA-9 Explosive Modeling Task of NASA's Second-Generation Reusable Launch Vehicle program.

The objective of this analysis was to characterize the explosive-hazard environment that may develop in the region of the launch pad due to the accidental and catastrophic release of the fuel and oxidizer from the booster and orbiter tanks for concepts of the second-generation shuttle launch system. Candidate configurations for the second-generation shuttle launch system consisted of a booster and orbiter in piggyback and/or axially mounted layouts (see Fig. 1). Boosters and orbiters such as those used by the current space shuttle launch vehicle system contain large tanks filled with liquid hydrogen (LH_2), liquid oxygen (LOX), and/or kerosene [rocket propellant (RP)]. Although structurally strong, these fuel tanks can lose structural integrity due to over pressurization of the tank (resulting in a catastrophic failure) or localized penetration from fragments, resulting from engine component failure on the launch pad. Whatever the initiation process may be, release of these fuels and oxidizer will create a potentially significant explosive-hazard potential, for which a subsequent explosive detonation will place the crew module and surrounding structures in a potentially lethal environment due to blast overpressure, thermal loads, and fragment impact. In addition, the use of solid rocket boosters introduces another source of blast overpressure and fragment fields, due to their potential catastrophic failure, that may also load or impact the crew module or may again result in subsequent failure of booster and orbiter tanks.

In this analysis, three specific quantities were predicted through computational simulation: 1) the magnitude and spatial extent of fuel–oxidizer mixing before explosive ignition in the on-pad region, 2) the corresponding magnitude of potential explosive yield resulting from detonation of the released species, and 3) the blast-field environment, including characteristics of fragments created by failure of vehicle components due to blast overpressure. In the approach used in this study, computational fluid dynamics (CFD) and hydrocode simulations were completed for different aspects of the problem. CFD simulations (using the FLOW-3D code [1]) predicted the predetonated explosive environment, which then served as the initial conditions for fluid–structure interaction simulations using the hydrocode CTH [2] (the name CTH is not an acronym). This paper then focuses on a methodology developed and applied for the computational simulation and prediction of explosive-hazard potential of the fuel and oxidizer releases in the vicinity of a launch vehicle system. Based on this methodology, the threat posed to the crew and crew module due to explosively generated overpressure and fragments is predicted and may then be used to design sufficient crew-escape features into launch vehicle systems.

A computational approach was taken in this effort because existing design methods for crew-escape systems based on simplified analytic solutions and very limited experimental or field data were deemed inadequate by the launch vendors. Thus, this methodology was formulated and uses existing verified and validated computational tools.

II. Background

A limited amount of research on unconfined vapor-cloud explosive hazard for LH_2 or RP vapor clouds has been reported in the open literature. To the authors' knowledge, no numerical or analytical work has been reported in which the modeling of the combined effects of 1) release of the fuel and oxidizer, 2) subsequent mixing of the fuel and oxidizer, and 3) prediction of the explosive potential and yield from the mixture plume were performed.

Typically an explosive-hazard analysis or assessment is performed to determine the potential for and the magnitude of candidate accident scenarios during launch operations. Historically, estimates of explosive yield for launch vehicles have relied on the

Received 11 July 2007; revision received 26 February 2008; accepted for publication 6 March 2008.

*Senior Program Manager, Computational Mechanics.
†Senior Research Engineer, Computational Mechanics.

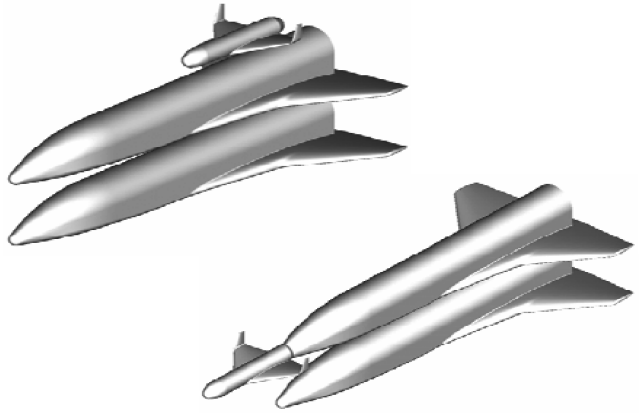

Fig. 1 Examples of candidate second-generation shuttle launch vehicles.

standard practice of using a "TNT (trinitrotoluene) equivalency," in which the blast wave is gauged using an equivalent mass of TNT (see Sec. VII for an additional discussion). Before 1971, the TNT equivalency criterion for LOX/LH_2 propellant for the static on-pad phase of the space shuttle launch operation was set at 60% of the onboard propellant mass (60% of approximately 1800 Mg). In 1971 [3], this percentage was reduced to 20% of TNT equivalency. The justification for this reduction was due to results from several experimental studies completed in the 1960s. The most relevant of these to this study was Project Pyro [4], in which bulkhead rupture and simulated vehicle fallback accident scenarios were experimentally reproduced for propellant masses of 90 to 41,000 kg. For these tests, the percent of TNT equivalency ranged from 0.05 to 100%; in general, as the propellant mass increased, the percent of TNT equivalency was reduced. The primary reason for this is the efficiency of the mixing process for smaller volumes; that is, it is easier to mix small-mixture volumes than large volumes. Recent work [5] has confirmed the use of a reduced percent of TNT equivalency for liquid propellants. In [5], for propellant masses ranging from 204 to 1000 kg, the percent of TNT equivalence was generally measured to be no more than 6%, although one test case achieved a magnitude of 35%. Today, most explosive-hazard assessments generally rely on the U.S. Department of Defense (DOD) standard in [6], which provides guidelines for assessing explosive hazard for launch vehicle systems. It is based on a historical review of launch vehicle explosions. The standard indicates an effective yield of 10% of TNT equivalence for LOX/LH_2 propellants and 14% for LOX/RP or LOX/LH_2/RP systems. These percentages are of the total propellant mass for the launch vehicle and thus may represent a significant amount of explosive mass.

III. Method

The methodology developed here is based on three phases of analysis and is illustrated in Fig. 2. The first phase of the method studies the spatial and temporal mixing of the fuel and oxidizer through the use of CFD simulations. The outcome of this effort is a prediction of the amount of fuel released, the spatial extent of the mixed region, and the local quality of the mixture cloud, all as a function of time. The second phase of the methodology calculates the yield potential of the mixture at each node in the computational grid system. In this analysis, a chemical-thermodynamic equilibrium computer code, (Cheetah) [7], is used to determine the explosive yield as a function of mixture quality. The functional relationship of mixture quality and yield is then used in a postprocessing mode to determine the mixture's yield potential over the spatial extent of the cloud and as a function of time. Because of the variable mixture quality of the vapor plume, some parts of the cloud are close to a stoichiometric mixture, whereas other regions are lean or rich and thus contribute less to the overall explosive yield. The third and last phases of this method then uses the time-dependent yield maps to

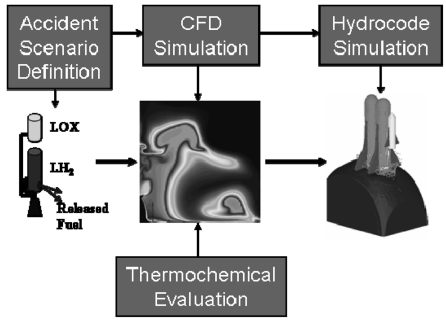

Fig. 2 Computational approach.

create an explosive mixture that may be either represented as a distributed explosive or as an equivalent condensed explosive, typically a spherical charge with a TNT equivalence. The equivalent condensed explosive has its center located at the center of mass of the plume and its radius is based on the weighted total explosive mass in the cloud, in which the weighting is based on mixture quality or explosive yield per computational cell. The mixture quality is determined based on the predicted mass percentages of the fuel and oxidizer in each computation cell. Simulations of the detonation of the resulting explosive mixture are then performed using CTH, which predicts blast pressures on the vehicle. In addition, the characteristics of fragments (size and velocity) are predicted based on the strain response of the launch vehicle's structural materials and the failure of these structures due to blast loading.

In this analysis procedure, the thermochemical Cheetah code [7] is used to estimate the explosive potential of hydrogen–air, hydrogen–oxygen, RP–air, and RP–oxygen mixtures. Cheetah solves the thermodynamic equations between product species to find chemical equilibrium. A simulation of detonation (a standard run) in Cheetah is based on Chapman–Jouget (C-J) detonation theory and considers a one-dimensional detonation. The transformation of the explosive to detonation products is assumed to occur very fast at steady-state when compared with hydrodynamic timescales. Based on this assumption, the state immediately behind the shock front then lies on the shock Hugoniot of the explosive product's equation of state. The Hugoniot is a curve of shock states in pressure-specific volume space that expresses conservation of mass, momentum, and energy across the shock front. C-J theory then postulates that the steady-state detonation occurs at the point of tangency between the Rayleigh line (which is an expression of the conservation of mass and momentum) and the release adiabat. Cheetah calculates the C-J state and then predicts the adiabatic expansion of the product gases from the C-J state down to 1 atm or a temperature of 298 K (whichever is reached first). The results are then fit to a Jones–Wilkins–Lee (JWL) equation of state [8]. The resulting JWL equations of state are then used as input to the CFD and hydrocode simulations to estimate explosive yield as a function of mixture quality. A series of Cheetah simulations are performed for different mixture mass ratios for each mixture. From these simulations, the functional relationship between explosive yield and mixture mass ratio is determined. Figure 3 displays this relationship for air–hydrogen and oxygen–hydrogen mixtures. The peaks of these curves represent the stoichiometric condition for the mixture, in which an air–hydrogen mixture mass ratio of 34.4:1 results in a maximum energy yield at detonation of 3.14 kJ/g, whereas a mass mixture of oxygen–hydrogen of 8:1 results in a maximum energy yield of 12.6 kJ/g.

When a flammable mixture is heated to an elevated temperature by an ignition source, a reaction is initiated that may proceed with sufficient speed to ignite the mixture to a self-sustaining condition. Typically, there is a time lag between the instant that the ignition source begins to elevate the local temperature of the mixture to when the mixture combusts, and this time lag is a function of the strength of the ignition source. Once the mixture is ignited and the resulting flame is self-sustaining, the flame will either attach itself to the ignition source or propagate through the mixture cloud. If the propagation speed is subsonic (based on the unburned mixture

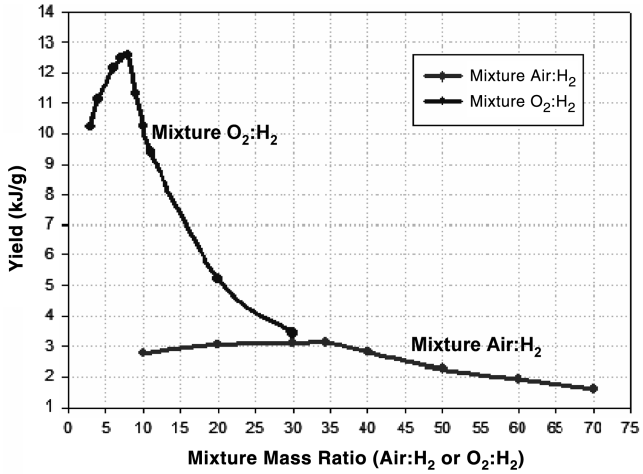

Fig. 3 Energy release or explosive yield for mixtures of air or oxygen with hydrogen.

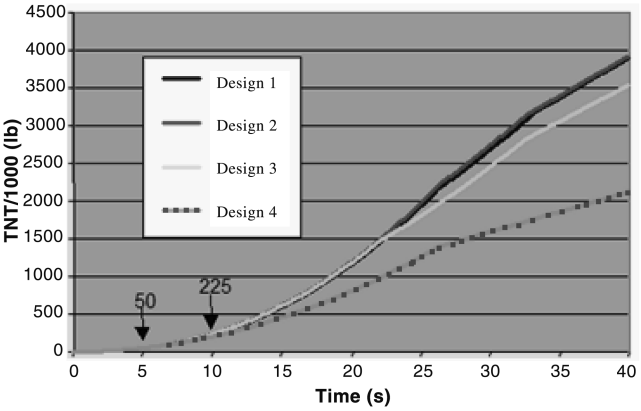

Fig. 4 Analytically determined TNT equivalency for four candidate RLV designs for a scenario-3 accident.

properties), then a deflagration results, and if the propagation speed of the flame front is supersonic, then the mixture has detonated. In the case of a deflagration, the flame-front propagation is slow enough to allow for pressure equalization to occur across the front and thus the overpressure due to a deflagration tends to be small (overpressure ratios up to 10:1) [9]. However, in the case of a detonation, insufficient time is available to achieve pressure equilibrium across the flame front, allowing for the pressure shock front to detach from the flame front. The flame front lags behind the shock front sufficiently to allow it to achieve local pressure equilibrium. The result is that the overpressure due to a detonation is significantly greater than in a deflagration, with overpressure ratios of up to 45:1 [9]. Note that a deflagration may transition to a detonation, but this is dependent on the mixture quality, temperature, pressure, ignition source, and geometry. Data for hydrogen explosions [5] suggest that a detonation does not occur, but rather that energy is released through a rapid deflagration. In this analysis, we assume that a detonation occurs (a conservative assumption) and we transform the mixture cloud to an equivalent TNT condensed-phase explosive (based on energy) that is then detonated.

IV. Evaluation of Accident Scenarios

The extent of fuel–oxidizer mixing in the predetonation environment and the resulting magnitude of potential explosive yield are discriminators that may be used to determine worst-case accident scenarios for a set of candidate designs. In this study, three accident scenarios were evaluated to define the worst-case accident scenario(s) to be simulated, as shown in Fig. 2. To reduce the number of detailed analyses or simulations to be performed, a prescreening of the design candidates was completed. This prescreening was executed using simplified analytic models for the processes, consistent with the physics of the accident scenarios and release processes. Complete details of this prescreening procedure are provided in [10]. However, briefly, the procedure accounts for two release processes: that of catastrophic tank failure (unzipping of a fuel–oxidizer tank) or localized tank rupture resulting in the release of a liquid jet. Analytic models for conductive and/or convective heat transfer and phase change are used to determine the rate of vapor-cloud formation. The yield potential is determined assuming ideal mixing, resulting in a stoichiometeric mixture.

Given the two release processes, the time sequence of release is based on three accident scenarios:

1) Scenario 1 is booster-engine failure with loss of thrust, resulting in the vehicle vertically settling back on the pad, with successive failure of the fuel and oxidizer tanks in the booster and orbiter due to impact with the pad structure.

2) Scenario 2 is LOX tank overpressure resulting in LOX tank rupture, leading to loss of thrust and causing the vehicle to vertically settle back on the pad, with successive failure of the fuel and oxidizer tanks in the booster and orbiter due to impact with the pad structure.

3) Scenario 3 is booster-engine catastrophic failure while the vehicle is on the pad (no vertical acceleration), leading to the simultaneous rupture or severing of the fuel and oxidizer feed lines, and resulting in the release of fuel–oxidizer as liquid/vapor jets.

Based on this prescreening procedure, it was concluded that scenario-3 feed-line rupture resulted in the greatest hazard potential for the candidate designs (fuel was LH_2). Further, it was found that there was very little difference between candidate launch vehicle configurations, in terms of TNT equivalence, for elapsed times from release less than approximately 10 s. An elapsed time of 10 s was considered to be the maximum time for operational response to the failure. That is, 10 s is the maximum time required to initiate and complete a crew-escape procedure so that the crew module will be sufficiently downrange from the event so that blast overpressure and fragment impact will be minimized on the crew module. For this accident scenario, the estimated explosive yield at 5 s after initiation of the accident event was 50,000 lb of TNT equivalent. By 10 s after initiation of the accident, the yield had increased to 225,000 lb of TNT equivalent. Figure 4 displays the time history for this worst-case accident event for four candidate designs (variants of candidates shown in Fig. 1). Note that all four designs have essentially the same release time histories up to approximately 10 s after initiation of the accident event. Differences between designs were due to location and orientation of the fuel–oxidizer tanks.

V. CFD Simulation and Analysis

A key element of any prediction of explosive potential is the need to evaluate the magnitude (spatially and temporally) of mixing of the various species under different release (accident) scenarios. Mixing is a transport process in which scalar quantities (e.g., temperature, momentum, chemical species, and particles) are distributed into the bulk flowfield through complex interactions of velocity gradients and physical parameters that are characteristic of the fluid. The intensity of the chemical reaction that results from detonation of a fuel and oxidizer is a strong function of the magnitude of mixing of the agents. In addition, mixing of the fuel and oxidizer will also control the time to detonation and the overpressure magnitude. From an explosive-hazards perspective, any mechanism that can either inhibit mixing of the fuel with the oxidizer (creating a too-rich fuel mixture) or allows for very rapid mixing (creating a too-lean fuel mixture) may be used to mitigate the hazard potential.

For example, the orientation of the fuel and oxidizer tanks in a launch vehicle will inhibit or augment mixing of the fuel and oxidizer for different release conditions. As already noted, LH_2 is stored at a significantly lower temperature than LOX, and LH_2 is always less dense than LOX at a given temperature. LOX will freeze when in contact with LH_2. Thus, if a LOX tank is located above an LH_2 tank (in a gravity field), then with simultaneous release as liquid jets, LOX will fall into and penetrate the released LH_2, causing the LOX to

freeze, whereas the buoyant LH_2 rises and maintains contact with the newly released LOX. This process results in significant liquid-phase mixing and increased explosive potential. If sufficient separation distance exists between the LOX and LH_2 release sites, then sufficient time may be available for both materials to transition to gas-phase, resulting in a buoyant hydrogen plume intersecting a denser oxygen plume and creating a significant explosive hazard due to gas-phase mixing. If, however, the LH_2 tank is located above the LOX tank (in a gravity field), then buoyancy effects do not enhance mixing and the LH_2 may not intersect or penetrate the denser LOX stream or plume.

To simulate the dynamic release and mixing of the fuel and oxidizer and to predict the resulting explosive yield of the forming vapor cloud based on yield-mixture curves, as shown in Fig. 3, the CFD code FLOW-3D is used. FLOW-3D is a commercial CFD code originally developed by Flow Science, Inc., and through a long-term relationship with Flow Science (more than 20 years), Southwest Research Institute has been involved in the development of elements of the code. FLOW-3D is a finite difference code based on the volume-of-fluid formulation for modeling two-fluid systems. It has a suite of physics modules for single- and multiphase fluids, with incompressible or compressible response. A set of turbulence models is available ranging from the standard k-ε model to a large eddy simulation model and each has supplementary terms to account for heat transfer effects. FLOW-3D solves for the time-dependent flow of fluids using a semi-implicit formulation with second-order formulations for spatial and temporal derivatives. In this application, the volume-of-fluid approach is used to track both the fuel and oxidizer (and the interface between them), and a renormalized group turbulence model is used to account for turbulent mixing.

The FLOW-3D code was validated against mixing problems (e.g., plume dispersion of a single species) similar to those studied here. Unfortunately, mixture quality data for fuel–oxidizer plumes does not exist, and thus we are not able to validate these predictions at this time; however, grid convergence tests performed in this study suggest that numerical uncertainty is relatively small (less than 10%) at these grid resolutions.

FLOW-3D was used to simulate the release and mixing of the fuel and oxidizer based on the scenario-3 accident previously discussed. The primary variables that were varied were the orientation of the released vapor jets (horizontal or vertical), the size of the rupture (0.5 or 1 m), the elevation of the rupture (15 or 30 m), and the wind speed (9.15 or 18.3 m/s) and direction (refer to Fig. 5). Figure 5 displays the definitions of some of these parameters for the scenario of an LH_2 tank rupture with a liquid/vapor jet discharging horizontally into a local atmosphere. The oxidizer in this case is the oxygen in the atmospheric air (see Fig. 3). Five different atmospheric states were studied: that is, a quiescent atmosphere and four different wind conditions, all for standard atmospheric conditions (one atmosphere and 20°C). Grid resolutions for these simulations ranged from 128,000 to 300,000, depending on the overall size of the domain. The grid resolution was determined by the diameter of the rupture, in which five zones were used across the diameter in all simulations. The grid was allowed to gradually expand to the boundaries of the domain.

Figures 6 and 7 are presented as examples of simulation results and display the extent of the mixed region of LH_2 and air after an elapsed time of 10 s for one of the five wind-field states (i.e., a velocity of 9.15 m/s or 30 fps moving from left to right in the image). Figure 6 displays the extent of the mixed region or total plume volume, and Fig. 7 displays the explosive-yield potential on the centerline of the plume. Clearly displayed in these two figures is the nonuniform quality or mixture mass ratio for the plume, which spans from a fuel-rich zone at the release site (low yield potential) to well-mixed regions near the leading edge of the plume. The wind field modifies the characteristics of the mixture plume in terms of spatial distribution. Positive wind fields shift the extent of the plume downwind and away from the vehicle, resulting in a separation from the vehicle of the center of mass of the explosive mixture. Negative wind fields force the plume to flow back on the vehicle and cause the center of the explosive mass to be centered on the vehicle and to thereby enhance the lethality of the explosive mixture to the launch vehicle system. Figure 8 displays a summary of the explosive-yield time histories for these four combinations of wind speed and direction, and included in this figure is the baseline condition for a quiescent wind-field state. Based on this study, both positive- and negative-direction wind fields augment the yield potential of the explosive mixture due to enhanced mixing resulting from the interaction of the wind and jet velocity fields.

As already discussed, the center of mass of the explosive-mixture plume is spatially altered by a wind-field condition. Thus, the magnitude of explosive-yield potential at an instant in time does not provide sufficient information to discriminate between the lethality of the plume resulting from various wind-field conditions. The necessary additional piece of information is the time history of the center of mass of the explosive mixture; these data are shown in Fig. 9. Two parameters then define the explosive-hazard potential for the launch vehicle (i.e., plume yield potential and location of the center of the plume mass). Blast overpressure at a specific location is a function of charge mass and separation distance between the location and charge mass center. Blast overpressure scales by the distance divided by the charge weight to the one-third power, and so overpressure scales more strongly on distance than on charge weight.

VI. Explosion Simulation and Analysis

The computational code used to simulate the detonation of the explosive mixtures and the collateral damage to the launch vehicle was CTH. CTH [2] is an Eulerian shock-physics wave-propagation code. This multidimensional Eulerian shock physics code, developed and maintained at Sandia National Laboratories, has the capability to model dynamic events that include explosive

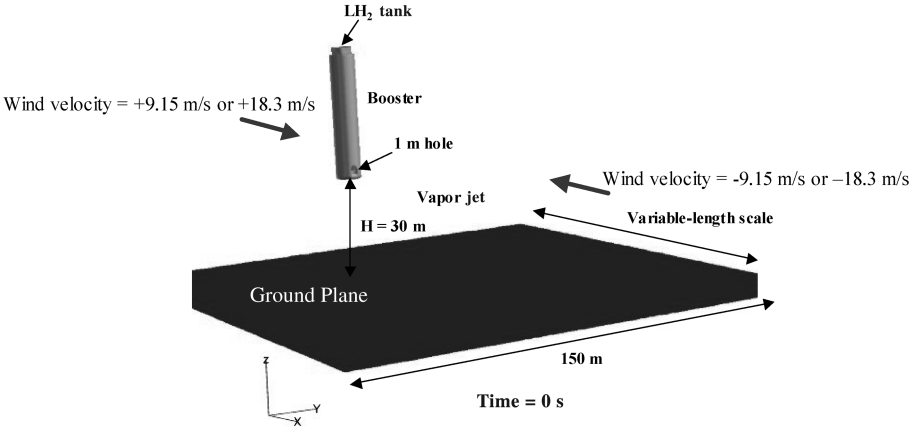

Fig. 5 CFD model geometry for a scenario-3 accident simulation.

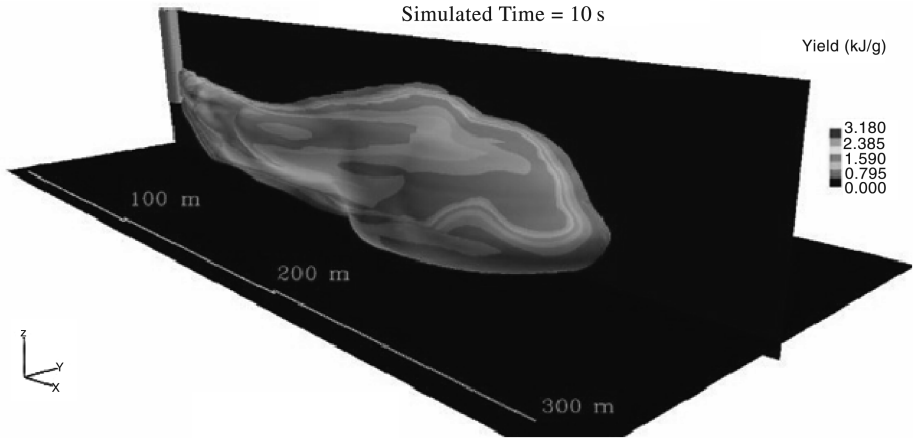

Fig. 6 Three-dimensional simulation of LH_2 released into a standard atmosphere with a 9.15-m/s (30-fps) wind field; simulated time is 10 s; shaded contours display yield intensity in kJ/g.

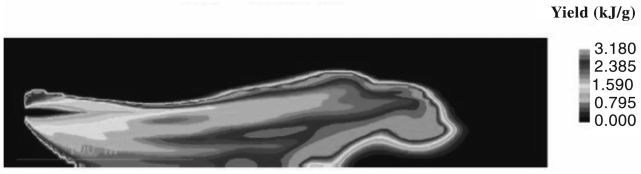

Fig. 7 Potential energy yield on centerline of plume shown in Fig. 6; shaded contours display yield intensity in kJ/g.

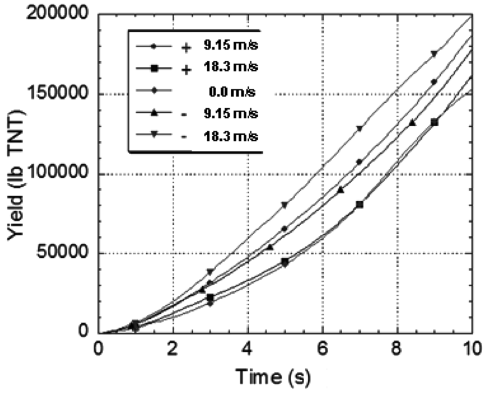

Fig. 8 Total potential yield based on CFD simulations for different environmental conditions.

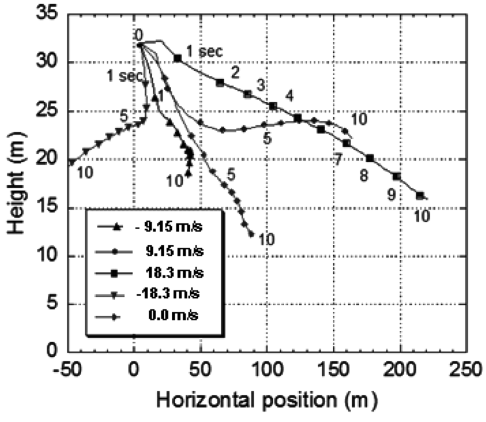

Fig. 9 Trajectories of center of mass for fuel–oxidizer vapor clouds.

detonation and high-velocity impact. The CTH code solves the differential equations describing conservation of mass, momentum, and energy during transient dynamic events on a fixed spatial mesh. CTH is capable of tracking the interactions of up to 20 materials. This code contains models suitable to describe material response under most conditions encountered in shock physics, including penetration, failure, sympathetic explosive response, and explosive energy release. Material response consists of an equation of state for the mean stress, a plasticity model for the deviatoric stresses, and a fracture model to insert a void into the grid system when the tensile stress has been exceeded. CTH also provides the ability to predict fragment formation and characteristics.

CTH has been verified and validated for a wide range of dynamic events, including detonation and blast effects. As illustration of this, a recently completed validation exercise by one of the authors for detonation of a condensed explosive in a partially confined space (a rectangular geometry with a three-sided structure and three open sides), is presented in Fig. 10. Here, a direct comparison of simulated and measured pressure–time histories is displayed. For the time period that the pressure transducers were functioning, the agreement between simulation and measured data is quite good. Field data from launch accidents, unfortunately, do not include pressure or impulse time histories or other data that may be used to validate a simulation. Validation of these detonation simulations against launch accidents has proved problematic due to the lack of appropriate data, and thus we have validated against other detonation events, as illustrated in Fig. 10.

Under loading conditions in which materials are undergoing expansion strain rates, it has been found that the characteristic dimension of the fragments that form can be determined by the strain rate at the time of fracture. Grady [11] derived the basic relationship between strain rate and the fragment dimensions:

$$S = \left(\frac{\sqrt{24}K_C}{\rho c \dot{\varepsilon}}\right)^{2/3}$$

where S is the average fragment size, K_c is the material fracture toughness, ρ is the material density, c is the material's speed of sound, and $\dot{\varepsilon}$ is the strain rate. Fragment characteristics are evaluated in the simulation, but do not couple back into the calculation to form discrete fragments [12]. As material is driven into expansion by the explosive overpressure, the divergent motion induces a strain rate that is then used to calculate S. The fragment dimension calculated by the preceding relationship is, as stated, an average. It is well documented that even under uniform strain rate, material will break into a distribution of fragment sizes. A Poisson distribution provides one method for describing the scatter about the mean size [12]. However, in the analysis performed here, only the average fragment size is reported.

Using the explosive-mixture state as determined in the previous section, the effects of detonation on a generic RLV vehicle are

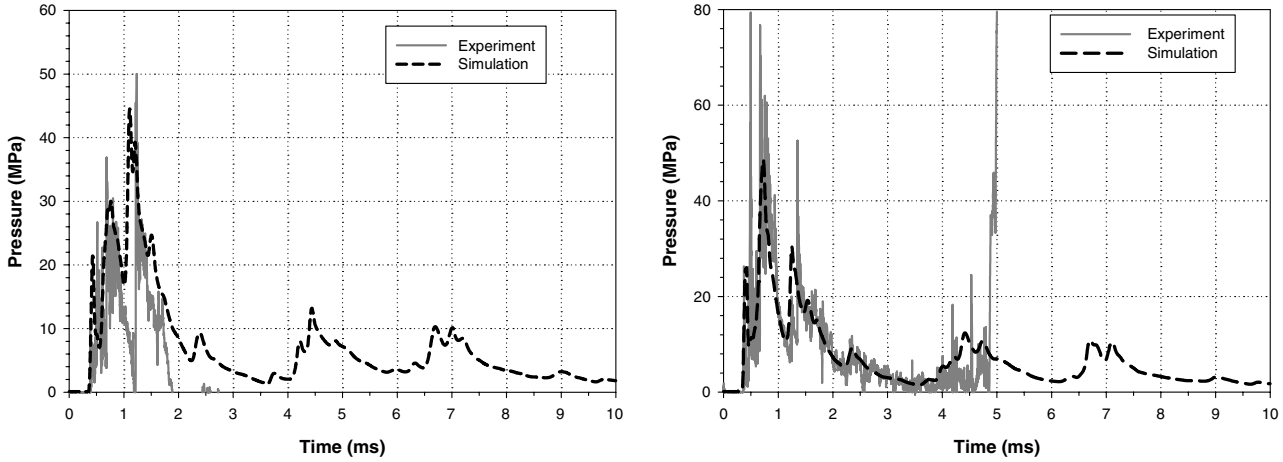

Fig. 10 Comparison of simulated and measured pressure–time histories resulting from detonation of a condensed-phase explosive.

modeled. The vehicle shell (substrate and insulation) is defined to be 10-cm thick, with a density of 0.061 g/cm^3, and give an areal density of 0.61 g/cm. The main wing components are defined to be of uniform thickness of 90 cm, with a density of 0.045 g/cm^3 and give an areal density of 4.05 g/cm^2. No support structures in the intertank or motor regions were included in the model. Four motors are modeled for both the booster and orbiter vehicles, and they were modeled as solid objects with a density of 0.5 g/cm^3. The crew module was also modeled as a solid body, being the potential target of the pressure and fragment field rather than a source. Table 1 provides a summary of the generic RLV characteristics.

Three-dimensional simulations were performed for different charge or explosive-mixture masses to study the pressure response near the crew vehicle and the fragment characteristics generated from booster and orbiter structures. The range of charge masses simulated accounted for cumulative releases of fuel (LH_2) of 1, 2, and 4 s, as predicted by the CFD simulations. The resulting explosive-mixture masses were then 4.5 Mg (10,000 lbm), 13.6 Mg (30,000 lbm), and 40 Mg (88,000 lbm), respectively. Figure 11 displays a sample illustration of the CTH simulation results for a 4.5-Mg mixture mass (modeled as a TNT equivalency). Grid resolution for these simulations ranged from 20–30 million zones [13]. Table 2 provides a summary of the results from these simulations, in which the fragment velocity range lists three values. The middle number represents the threshold above which a small percentage (less than 5%) of the fragments have velocities greater than this threshold and up to the maximum velocity, which is defined by the third number.

Table 1 Characteristics of a generic RLV

Item	Mass or length
Overall length	47 m
Diameter	8.9 m
Wingspan	28 m
LH_2 mass	110 Mg
LOX mass	612 Mg
Wing mass	11 Mg
Motor mass (per motor)	3.7 Mg
Structure mass	19 Mg
Total vehicle mass	771 Mg

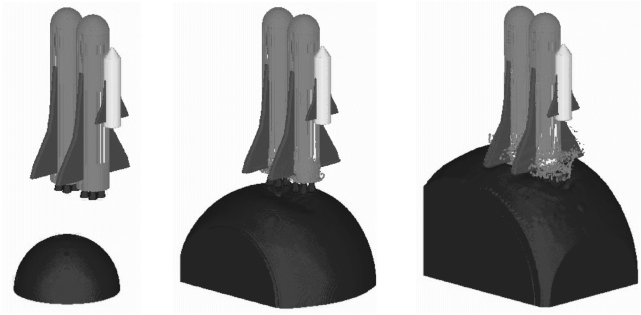

Fig. 11 CTH simulation results for detonation of a 4.5-Mg explosive mixture with a generic RLV; images are at times of 0, 50, and 100 ms, respectively (moving from left to right).

The arrival time is the time at which the peak overpressure reaches the crew module.

VII. Conclusions

Throughout this paper, the explosive-hazard potential was reported in terms of TNT equivalence. This is a standard practice and was done here to provide a common scaling or reference and to thereby provide a common understanding of the relative magnitude of the explosive-hazard potential. However, one should not misinterpret what TNT equivalence means or lose sight of the limitations of this scaling. TNT equivalence, as used here, simply converts the mass of the explosive mixture to an equivalent mass of TNT, scaled by detonation energy. This is intended to allow the interpretation that the blast waves generated by the explosive mixture and an equivalent TNT mixture are self-similar. However, formally, self-similar response requires two charges of similar geometry, of the same explosive material (but of different sizes), and detonated in the same atmosphere. The requirement of the explosive charges being of the same material is a critical issue, because the response or energy release of a condensed explosive such as TNT is different from that for a diffuse explosive mixture such as hydrogen and oxygen. The significance of this is that the near-field or close-in response from the detonation of an equivalent mass of TNT will be more energetic than

Table 2 Summary of Results from CTH Simulations

Explosive mass, kg (lb)	Peak overpressure, MPa (psi)	Arrival time, ms	Fragment velocity range, m/s	Fragment size range, cm (in.)
4536 (10,000)	0.21 (30)	72	50–100–400	25.4–76.2 (10–30)
13,608 (30,000)	0.41 (60)	54	50–150–500	22.9–76.2 (9–30)
39,916 (88,000)	1.1 (160)	37	50–250–600	22.9–50.8 (9–20)

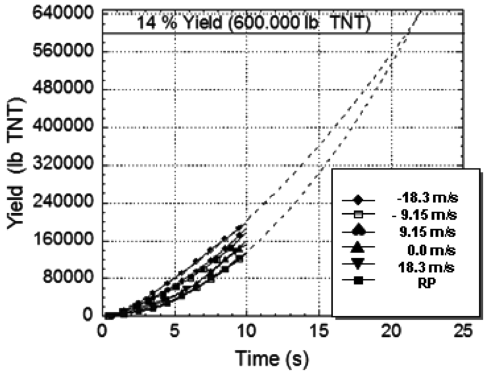

Fig. 12 Extrapolated explosive-yield curves of L H_2 and RP fuel mixing with air.

that for the gaseous mixture, due to the rate at which each explosive material releases energy. However, in the far field, and assuming that the same total energy has been released (but over a different timescale), then the blast-pressure waves will tend to be self-similar and, in fact, will be almost identical in the far field, because the total energy released by the explosives is the same.

Finally, based on this type of analysis, an assessment of the conservatism in the DOD standard in [6] for explosive potential hazard analysis for launch vehicles may be demonstrated. For LH_2/LOX/RP configurations, the DOD standard [6] recommends that the potential yield should be estimated as the greater of 14% or 8 $W^{2/3}$, where W is the total propellant weight. The 14% threshold may be representative of the yield resulting from the primary detonation plus all subsequent, secondary, detonations, but is not necessarily representative of the primary hazard potential. Figure 12 displays the predicted primary hazard potential due to the accident scenarios studied here and includes the 14% criteria as a threshold value. The value of 272 Mg (600,000 lbm) of TNT equivalent is based on an RLV system consisting of a booster and orbiter configuration. To achieve the 14% threshold would then require an elapsed time of over 20 s to release and disperse the fuel mass into an explosive mixture. The analysis presented here suggests that the 14% criterion considerably overestimates the potential yield of the primary detonable mixtures for these accident scenarios and in terms of crew escape. A crew-escape system designed based on the 14% criterion would appear to have a significant level of conservatism built into the design.

References

[1] FLOW-3D, Software Package, Ver. 9.0, Flow Science, Inc., Sante Fe, NM, 2005.

[2] McGlaun, J. M., Thompson, S. L., and Elrick, M. G., "CTH: A Three-Dimensional Shock Wave Physics Code," *International Journal of Impact Engineering*, Vol. 10, Nos. 1–4, 1990, pp. 351–360. doi:10.1016/0734-743X(90)90071-3

[3] Wolfe, R. R., "Final Report: TNT Equivalency Study for Space Shuttle (EOS), Volume 1: Management Summary Report," NASA CR-123370, Sept. 1971.

[4] Willoughby, A. B., Wilton, C., and Mansfield, J., "Liquid Propellant Explosive Hazards," U.S. Air Force Rocket Propulsion Lab., TR-68-92, Edwards AFB, CA, Dec. 1968.

[5] Bunker-Farrah, R. L., Eck, M., Taylor, J. W., and Hancock, S., "Correlation of Liquid Propellants," NASA Johnson Space Center, White Sands Test Facility, WSTF-TR-00985-001-01-02, Las Cruces, NM, Sept. 2002.

[6] "DOD Ammunition and Explosives Safety Standards," U.S. Department of Defense Standard 6055-9-STD, July 1999.

[7] Cheetah, Software Package, Ver. 5, Lawrence Livermore National Lab., Livermore, CA, 2007.

[8] Wilkins, M. L., *Computer Simulation of Dynamic Phenomena*, Springer–Verlag, Berlin, 1999, pp. 75–81.

[9] Gugan, K., *Unconfined Vapor Cloud Explosions*, Gulf, Houston, TX, 1979.

[10] Freitas, C. J., Chocron, S., Cox, P. A., and Bernardo, A. B., "Explosive Environment Modeling Study—2nd Generation RLV Systems Engineering and Risk Reduction Program," Southwest Research Inst., San Antonio, TX, May 2003.

[11] Grady, D. E., "The Spall Strength of Condensed Matter," *Journal of the Mechanics and Physics of Solids*, Vol. 36, No. 3, 1988, pp. 353–384. doi:10.1016/0022-5096(88)90015-4

[12] Kipp, M. E., Grady, D. E., and Swegle, J. W., "Numerical and Experimental Studies of High-Velocity Impact Fragmentation," *International Journal of Impact Engineering*, Vol. 14, Nos. 1–4, 1993, pp. 427–438. doi:10.1016/0734-743X(93)90040-E

[13] Kipp, M. E., and Saul, W. V., "Fragment and Pressure Environments from Propellant Explosions in Reusable Launch Vehicle Near-Pad Accidents," Sandia National Labs., Rept. SAND2003-0652, Albuquerque, NM, Mar. 2003.

A. Ketsdever
Associate Editor